Viscosity of bubble and crystal-bearing silicate melts

Joachim Deubener
Institut für Werkstoffwissenschaften und -technologien, Technische Universität Berlin, Englische Strasse 20, D-10587 Berlin, Germany

Viscosity of bubble and crystal-bearing silicate melts is studied for isochemical systems in the range of linear and non-linear viscous flow. For crystal bearing melts effects on viscosity are characterised by volume fraction and morphology of suspended crystals. Whereas dispersed crystals increase the viscosity, alignment of crystals is attributed to shear thinning. In the case of bubble-bearing silicate melts the importance of bubble deformation is characterised by the capillary number Ca. For Ca >>1 bubbles readily deform and viscosity decreases. Shear thinning caused by bubble deformation is restricted to rheodynamic regimes with Ca values close to unity.

Introduction

Viscosity is a key property of glass fusion and processing. While forming of glass is mostly restricted to homogeneous (single-phase) liquids, heterogeneous (multi-phase) melts are involved in processing glass-ceramics for high technology applications, including dental restorations[12], optical connectors[3] and fiber materials[4]. Increasingly interest on flow properties of multi-phase melts evoke since these products are drawn and pressed from partially crystallised pre-forms. Moreover, if glass is fused from batch materials transitional multi-phase liquids occur as the raw materials melt gradually accompanied by bubble formation of entrapped gases and volatile decomposition products. Besides this, magmas and lavas typically contain crystals and bubbles suspended in a liquid[56] Thus, understanding the mechanisms underlying the flow of heterogeneous melts is critical to development of models for fusion and processing of synthetic glass products and for predicting geophysical processes. This paper summarises the main effects of bubbles and crystals on the suspension viscosity which were studied previously by cylinder compression experiments.

Flow of homogeneous silicate melts

Single-phase silicate melts usually behave as Newtonian fluids if the strain or strain rate $\dot{\varepsilon}$ is low. However, non-Newtonian or strain rate-dependent viscous flow at high deformation rates for shear[7], tensile[8] and compressive stresses[9] is observed (Fig.1).

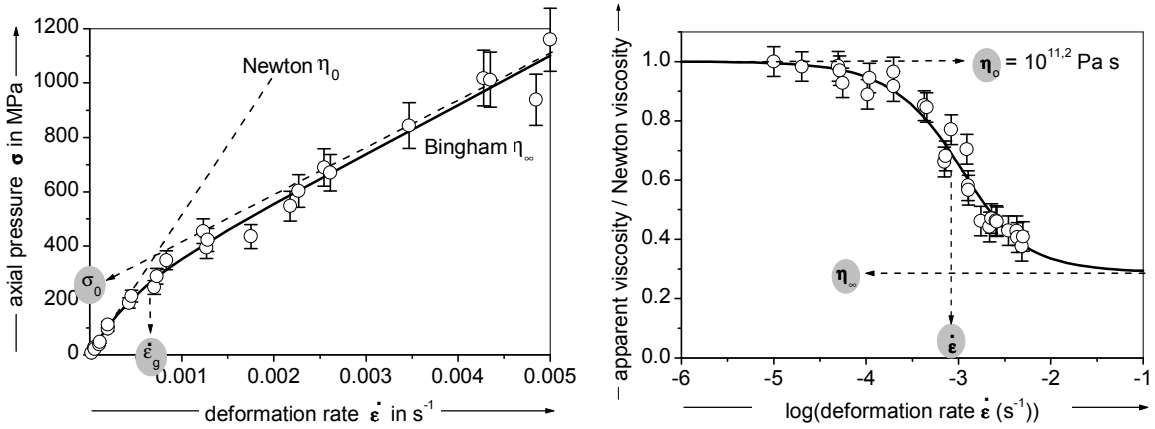

Fig. 1: Flow curve (left) and normalised apparent viscosity (right) of an inclusion-free lithium disilicate melt under compressive conditions at T = 468°C[10].

The flow curve in Fig. 1 can be interpreted as a combination of a Newtonian flow at low deformation rates and a Bingham flow at high deformation rates connected by a relaxation function with the flow relaxation rate $\dot{\varepsilon}_g$. The Yue-Brückner equation is used to describe shear thinning of an inclusion-free homogeneous glass melt[11]:

$$\eta_{app} = \frac{\sigma}{m\dot{\varepsilon}} = \eta_\infty + \frac{\sigma_0}{m\dot{\varepsilon}}\left[1 - \exp\left(\frac{-\dot{\varepsilon}}{\dot{\varepsilon}_g}\right)\right] \qquad (1)$$

with η_{app} = apparent viscosity, σ = axial stress, $\dot{\varepsilon}$ = strain rate, m = geometric factor for shear, tensile and compressive experiment, η_∞ = ultimate viscosity, $\dot{\varepsilon}_g$ = flow relaxation rate. Non-Newtonian flow is assumed to depend on viscoelastic relaxation of stresses which are produced by dynamic orientation effects of structural units (e.g. chains, discs or network fragments) in the glass melt[12]. Orientation effects induced by a forced flow are observed as birefringence[13], mechanical anisotropy[14] and by structural investigations[15].

Flow of crystal-bearing silicate melts

Newtonian flow is limited to low and moderate crystal volume fractions. The onset of a yield strength is a function of crystal shape and orientation distribution. Critical values of the crystallinity are reported to be in the range from 20 to 35 vol%[5] which is consistent with results of numerical simulations[16]. Within the range of rate independent flow viscosity can be studied under isothermal and isochomal conditions (Fig. 2).

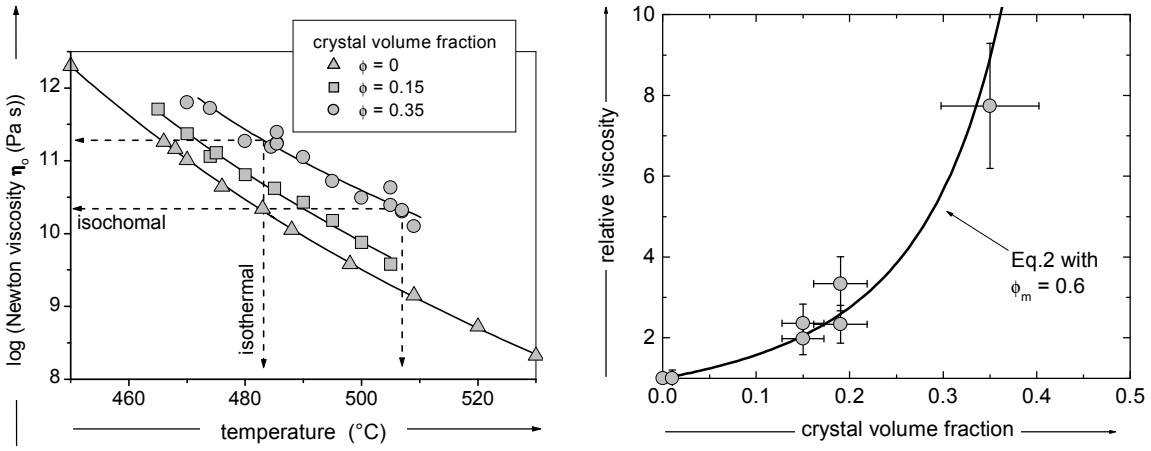

Fig. 2: Effective Newtonian viscosity as a function of temperature (left) and crystal fraction (right) of isochemical crystal-melt suspensions with lithium disilicate composition.[10]

On isothermal conditions the Einstein-Roscoe equation is often used to take into account effects of interacting, non-colloidal rigid inclusions[17]:

$$\eta_{rel} = \frac{\eta_{susp}}{\eta_{0,m}} = \left(1 - \frac{\phi}{\phi_m}\right)^{-2.5} \qquad (2)$$

with η_{rel} = relative viscosity, η_{susp} = effective viscosity of the suspension, $\eta_{0,m}$ = Newtonian viscosity of the suspending liquid, ϕ = crystal volume fraction, ϕ_m = maximum packing fraction.

Additional shear thinning at moderate deformation rates is observed if the flow curve of a partially crystallised melt is inspected (Fig.3). This effect is attributed to rotation and elastic interaction of non isometric crystals. Thus, crystal alignment can be used to produce oriented glass-ceramic materials[18]. To separate shear thinning which is attributed to dispersed crystals from non-Newtonian flow caused by suspending liquid one may deconvolute the curve of the apparent viscosity assuming superposition of two separate flow equations[10]:

$$\eta_{app} = \eta_{appl} + \eta_{app2} = \eta_{\infty 1} + \frac{\sigma_{01}}{m\dot{\varepsilon}}\left[1 - \exp\left(\frac{-\dot{\varepsilon}}{\dot{\varepsilon}_{g1}}\right)\right] + \eta_{\infty 2} + \frac{\sigma_{02}}{m\dot{\varepsilon}}\left[1 - \exp\left(\frac{-\dot{\varepsilon}}{\dot{\varepsilon}_{g2}}\right)\right] \quad (3)$$

In Eq. (3) the index 1 and 2 denotes shear thinning caused by the suspended crystals and the liquid matrix, respectively.

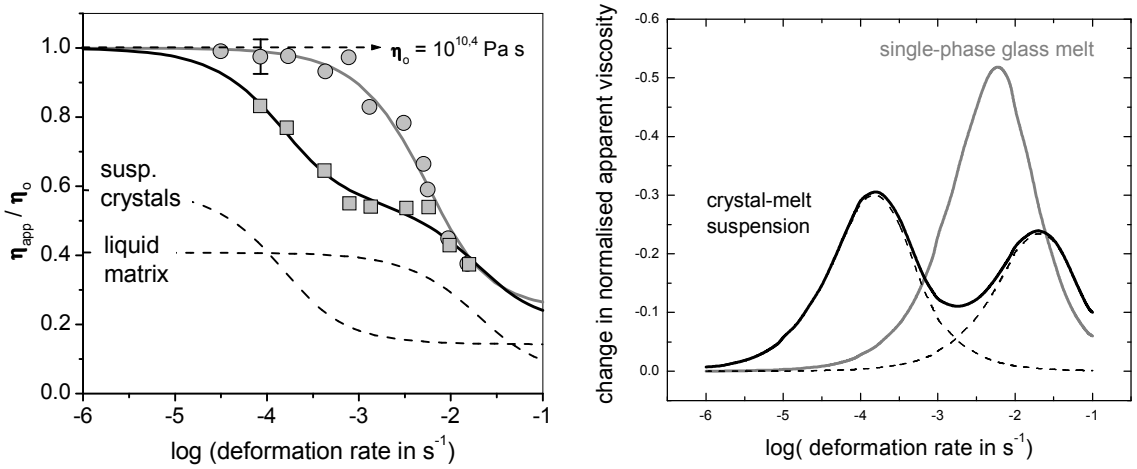

Fig. 3: Normalised apparent viscosity of a partially crystallised melt (square, f = 0.19) and a inclusion-free melt (circle) of lithium disilicate composition for isochomal temperature T10.4 (η_0=$10^{10.4}$ Pa s) (left)[19]. First derivative, $d(\eta_{app}/\eta_0)/d(\log(\dot{\varepsilon}))$ (right).

One may use the first derivative to visualise the change in viscosity with variation of the deformation rate and to find the location of the flow relaxation rate of the liquid matrix and suspended crystals (peak maximum) (Fig. 3). Latter is a function of the crystal morphology (aspect ratio a:b:c). Deconvolution of the viscosity curve shows that with increasing deviation from the isometric form the onset of shear thinning shifts to smaller deformation rates, i.e. smaller flow stresses. (Fig. 4).

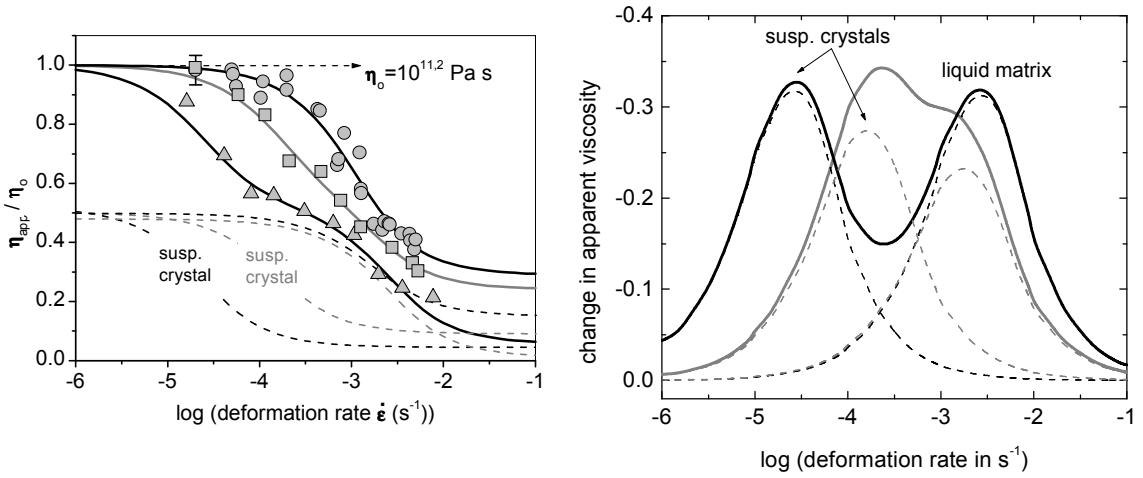

Fig. 4: Normalised apparent viscosity of two partially crystallised melts with different crystal shape (square: $\phi = 0.15$, aspect ratio 1:1:1.5; triangle: $\phi = 0.15$, aspect ratio 2.4:1:3.9) and of the inclusion-free melt (circle) of lithium disilicate composition for isochomal temperature $T_{10.4}$ (η_0=10$^{10.4}$ Pa s) (left)[10]. First derivative $d(\eta_{app}/\eta_0)/d(\log(\dot{\varepsilon}))$ of the partially crystallised melts(right).

However, if the crystal volume fraction is modified and the crystal morphology is kept constant the location of the shear thinning maxima are preserved. In the case the crystallinity of a melt is increased by growing crystals to larger sizes total shear thinning is found to be increasingly dominated by the contribution of the suspended crystals (Fig. 5).

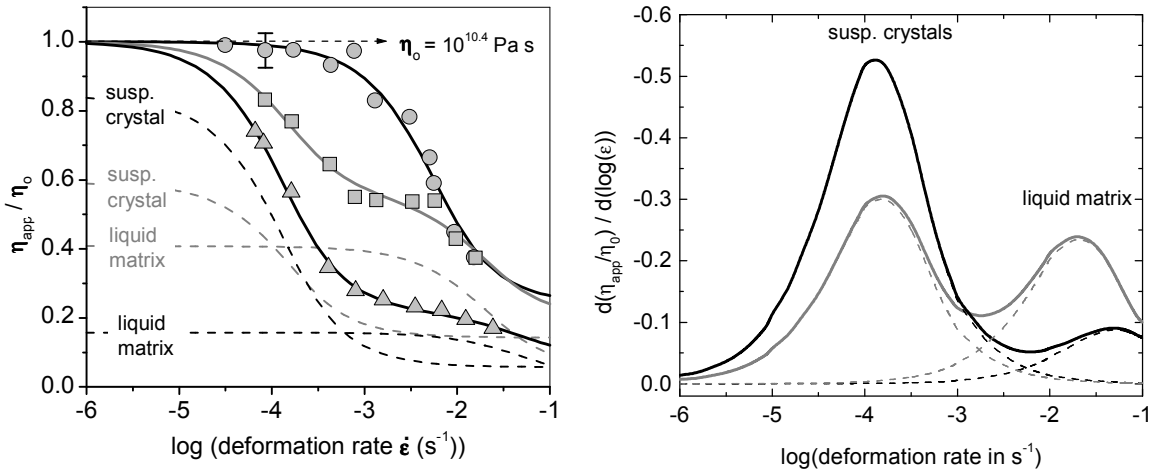

Fig. 5: Normalised apparent viscosity of two partially crystallised melts with different crystal volume fraction (square: $\phi = 0.19$, aspect ratio 2.3:1:3.8; triangle: $\phi = 0.33$, aspect ratio 2.4:1:3.9) and of the inclusion-free melt (circle) of lithium disilicate composition for isochomal temperature. First derivative $d(\eta_{app}/\eta_0)/d(\log(\dot{\varepsilon}))$ of the partially crystallised melts (right).

Flow of bubble-bearing silicate melts

On most conditions, strain rate-independent flow of bubble-bearing silicate melts is achieved. In this case bubbles act as deformable inclusions, i.e. the ratio of viscous forces acting on the boundary of the bubble distorting it to the interfacial tension that tries to preserve its spherical shape is large. These counteracting forces are characterised by the capillary number Ca[5]:

$$Ca = \eta_{app} \frac{r\dot{\varepsilon}}{\sigma} \qquad (4)$$

with r = bubble radius and σ = bubble-melt interfacial tension. Thus, for Ca >> 1 bubble deformation occur and viscosity is decreased, whereas for Ca << 1 bubbles remain spherically and viscosity of the bubble-bearing melt is greater than that of the suspending fluid. However in the range Ca ≈ 1 a strain rate-dependent viscosity (shear thinning) is expected since the behaviour of bubbles in viscous flow is changing from rigid to soft[5].Within the capillary number range from 10^3 to 10^5 (surface tension stresses are negligible) non-Newtonian flow of bubble-bearing silicate melts is restricted to the shear thinning caused by the liquid matrix (Fig. 6). In this case flow curves are self-similar and one may employ Eq. 1 for description.

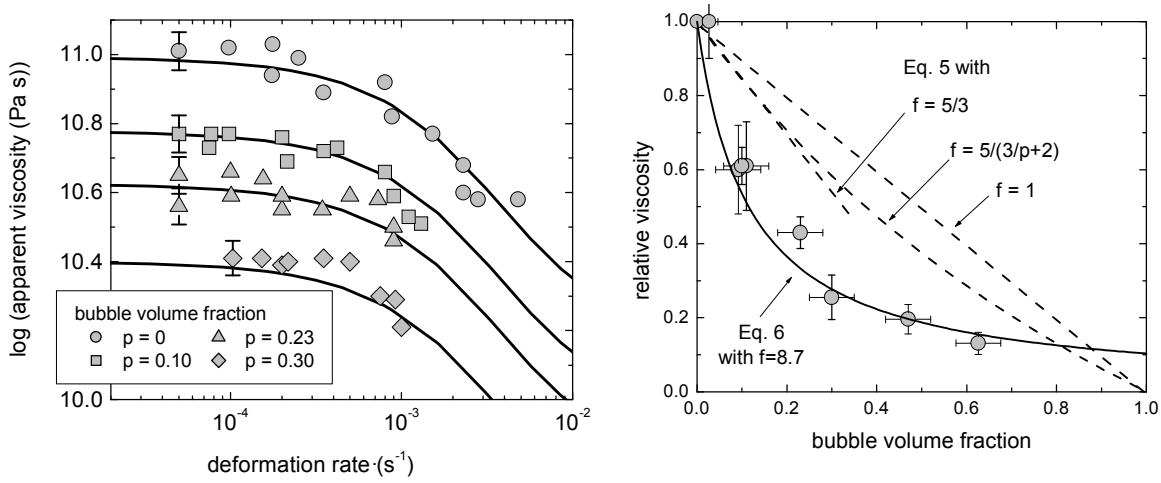

Fig. 6: Apparent viscosity of bubble-bearing silicate melts of float-glass composition at 574°C as a function of deformation rate (10^3 < Ca < 10^5) (left)[20] and bubble volume fraction (right).

Effective viscosity decrease with increasing bubble volume fraction. On isothermal conditions and for vanishing surface tension stresses it is assumed that bubbles do not affect the flow, i.e. viscous dissipation occurs only in the volume fraction which is occupied by the liquid phase (1-p). Thus, the relative viscosity of a bubble-bearing liquid can be written as:

$$\eta_{rel} = \frac{\eta_{susp}}{\eta_0} = 1 - f\,p \qquad (5)$$

with p = bubble volume fraction and f = 1 (dilute suspension: f = 5/3, Hashin-Shtrickman limit: f = 5/(3/p+2)). In contrast, Fig. 6 shows that effective viscosity of a bubble bearing melt with float-glass composition is better described by the empirically derived Bagdassarov-Dingwell equation[21]:

$$\eta_{rel} = \left(\frac{1}{1 + f\,p} \right) \qquad (6)$$

However, Eq. (6) is inconsistent with theory since for p = 0 the relative viscosity is not zero.

Flow of bubble and crystal-bearing silicate melts

On isothermal conditions and for Ca >>1 the flow curves of bubbly crystal-melt suspensions show two-step shear thinning with variable step heights, onset rates and Newtonian viscosities depending on the volume fractions and shape of each type of inclusions (Fig. 7). Eqs. (2), (3) and (6) are employed to calculate the effective viscosity of such a multi-phase silicate melt.

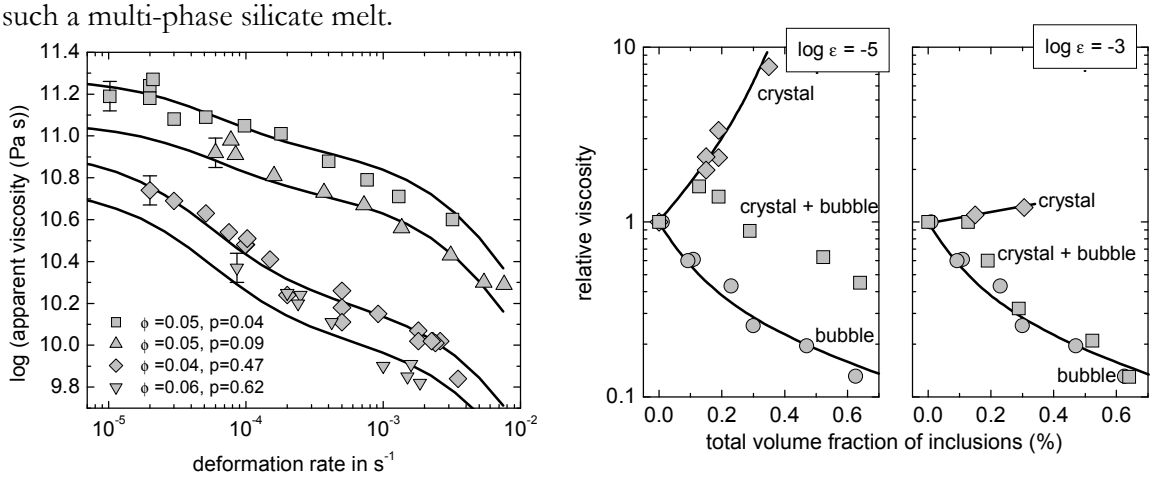

Fig. 7: Apparent viscosity of bubble and crystal-bearing silicate melts with float-glass composition at 574°C (left)[20]. Relative viscosity of multi-phase silicate melts for for $\dot{\varepsilon}$ = 10^{-3} and 10^{-5} (right)

The relative viscosity of a multi-phase silicate melts is within the limits of that of the pure crystal-melt and pure bubble-melt suspension. Thus, η_{app} can be larger or smaller than the apparent viscosity of the inclusion-free melt. However, these bounds depend strongly on deformation rate.

Conclusions

It is found that the effect of suspended crystals and bubbles on the viscosity of silicate melt is mainly a function of their volume fraction, shape and distribution if strain rate-independent flow is studied. In contrast, deformation, rotation and elastic interaction of the inclusions can cause strain rate dependent flow (shear thinning). It is shown that frequency scans or deformation rate studies are advantageous to separate contributions on viscosity of different types of inclusions.

Acknowledgements

I thank my collaborators Prof. R. Brückner, Prof. Y. Yue, Prof. M. Weinberg and M. Thies for their contributions, inspiration and comments in the performance of this work. Also, I am grateful for the support of the DFG.

[1] W. Höland, M. Frank, M. Schweiger, S. Wegner and V. Rheinberger, Glastech. Ber. Glass Sci. Technol. **69**, p. 25 (1996).

[2] M. Frank, V. Schweiger, V. Rheinberger and W. Höland, Glastech. Ber. Glass Sci. Technol. **71C**, p. 345 (1998).

[3] A. Sakamoto, S. Yamamoto in *19th Int. Congr. Glass,* 2001, Extended abstracts, p. 184.

[4] S. Yoo, U. C. Paek and W.T. Han, J. Non-Cryst. Solids **303**, p. 291 (2002).

[5] M. Manga, J. Castro, K.V. Cashman and M. Loewenberg, J. Volcanol. Geotherm. Res. **87**, p. 15 (1998).

[6] S.R. Hoover, K.V. Cashman and M. Manga, J. Volcanol. Geotherm. Res. **107**, p. 1 (2001).

[7] J.H. Simmons, R.Ocha, K.D. Simmons and J.J. Mills, J. Non-Cryst. Solids **105**, p. 313 (1988).

[8] J.H. Li and D.R. Uhlmann, J. Non-Cryst. Solids **3**, p. 127 (1970).

[9] P. Manns and R. Brückner, Glastechn. Ber. **61**, p. 46 (1988).

[10] J. Deubener and R. Brückner, J. Non-Cryst. Solids **209**, p. 96 (1997).

[11] Y. Yue and R. Brückner, J. Non-Cryst. Solids **180**, p. 66 (79).

[12] R. Brückner, Glastech. Ber. Glass Sci. Technol. **67C**, p. 161 (1994).

[13] A. Habeck and R. Brückner, J. Non-Cryst. Solids **162**, p. 225 (1993).

[14] R. Brückner, Glastech. Ber. Glass Sci. Technol. **69**, p. 396 (1996).

[15] R. Brückner in *8th Int. Congr. Glass,* 1965, Volume I.3.2 , p. 38.1.

[16] M.O. Saar, M. Manga, K.V. Cashman and S. Fremouw, Earth Planet. Sci Lett. **187**, p. 367 (2001).

[17] R. Roscoe, in *Flow properties of disperse systems*, edited by J.J. Hermans (Nort Holland, Amsterdam, 1953), p. 1.

[18] C. Rüssel, Glastech. Ber. Glass Sci. Technol. **73C1**, p. 162 (2000).

[19] J. Deubener and R. Brückner, Ber. Bunsenges. Phys. Chem. **100**, p. 1443 (1996).

[20] M. Thies and J. Deubener, Glass Technol. (In press)

[21] N. Bagdassarov and D.B. Dingwell, J. Volcanol. Geothern. Res. **50**, p. 307 (1992).